

# High DOF Tendon-Driven Soft Hand: A Modular System for Versatile and Dexterous Manipulation

Yeonwoo Jang<sup>1,\*</sup>, Hajun Lee<sup>1,4,\*</sup>, Junghyo Kim<sup>1</sup>, Taerim Yoon<sup>2</sup>, Yoonbyung Chai<sup>2</sup>, Heejae Won<sup>1</sup>  
 Sungjoon Choi<sup>2</sup> and Jiyun Kim<sup>1,3,†</sup>

**Abstract**—The soft robotic hand exhibits a wide range of manipulation capabilities, which are attributed to the dexterity of its soft fingers and their coordinated movements. Therefore, designing a versatile soft hand requires careful consideration of both the characteristics of the individual fingers, such as degree of freedom (DOF), and their strategic arrangements to improve performance for specific target tasks. This work presents a modularized high DOF tendon-driven soft finger and a customized design of a soft robotic hand for diverse dexterous manipulation tasks. Furthermore, an all-in-one module is developed that integrates both the 4-way tendon-driven soft finger body and drive parts. Its high DOF enables multi-directional actuations with a wide actuation range, thereby expanding possible manipulation modes. The modularity of the system expands the design space for finger arrangements, which enables the diverse configuration of robotic hands and facilitates the customization of task-oriented platforms. To achieve sophisticated control of these complex configurations, we employ neural network-planned trajectories, enabling the precise execution of complicated tasks. The performance of a single finger is validated, including dexterity and payload, and several real-world manipulation tasks are demonstrated, including writing, grasping, rotating, and spreading, using motion primitives of diverse soft hands with distinctive finger arrangements. These demonstrations showcase the system’s versatility and precision in various tasks. We expect that our system will contribute to the expansion of possibilities in the field of soft robotic manipulation.

## I. INTRODUCTION

Soft robots have been spotlighted owing to their potential for safe and robust manipulation of human-machine interface and machine-machine interfaces [1]–[3]. The use of soft robots as end-effectors in robotic hands is a particular noteworthy application. Their compliant and flexible characteristics enable stable and adaptive interactions with a diverse range of objects, accommodating different materials, shapes, and textures [4], [5].

This work was supported by National Research Foundation of Korea (NRF) grants funded by the Korean government (RS-2023-00302525, RS-2024-00407155, RS-2025-00564307, RS-2024-00358438), Korea Institute of Materials Science (KIMS) grants funded by KIMS (PNK8310), Institute of Information & Communications Technology Planning & Evaluation (IITP) grant funded by the Korean government (MSIT) (No. 2019-0-00079), Artificial Intelligence Graduate School Program (Korea University).

\* Corresponding author: Jiyun Kim. Email: jiyunkim@unist.ac.kr

† The authors contributed equally to this study

<sup>1</sup>Department of Materials Science and Engineering, Ulsan National Institute of Science and Technology, 50 UNIST-gil, Ulju-gun, Ulsan, Korea.

<sup>2</sup>Department of Artificial Intelligence, Korea University, 145 Anam-ro, Seongbuk-gu, Seoul, Korea. <sup>3</sup>Center for Multidimensional Programmable Matter, Ulsan National Institute of Science and Technology, 50 UNIST-gil, Ulju-gun, Ulsan, Korea. <sup>4</sup>Department of Mechanical Engineering, University of California, Berkeley, 2505 Hearst Ave, Berkeley, CA, 94709, USA.

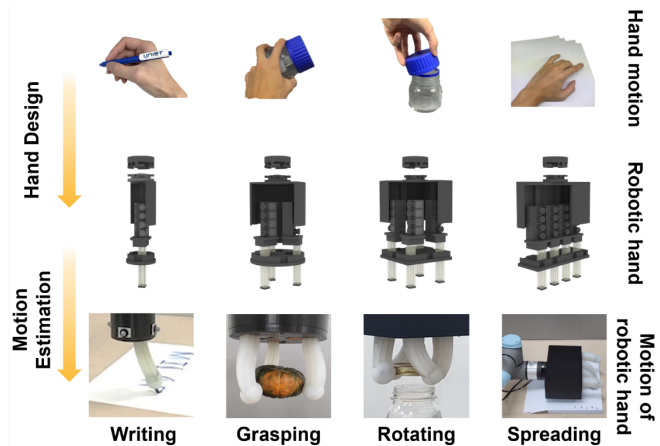


Fig. 1. Overview of the modular system. The design of the platform is guided by the configuration of common hand motions. Robotic hands are equipped with the soft finger modules, the designed platform, and a platform cover. Each of these hands demonstrates improved hand manipulation tasks, respectively, based on the platform’s design.

The performance of a soft robotic hand is contingent upon two key factors: (1) the dexterity of an individual finger and (2) the configuration of these fingers. The motion primitives of robotic hands stem from both the actuation of individual fingers and their cooperative motions. Thus, the development of an efficient soft hand necessitates the design of novel soft fingers with consideration for degree of freedom (DOF), material composition, and operation methods. Furthermore, the strategic arrangement of these fingers must be configured to enhance task-specific functionality.

The DOF is of paramount importance in defining the motion primitives available to robotic hands, particularly in the context of soft fingers, as depicted in Fig. 1. A high DOF allows for multi-directional operation and the creation of various actuations. This capability has motivated researchers to emulate the complex and flexible motions observed in natural organisms, including human hands [6], elephant trunks [7], and octopus tentacles [8]. The pursuit of high DOF actuation facilitates gentle and dexterous manipulation. Moreover, the increased DOF of the soft finger enhances design flexibility, reducing constraints on the assembly direction or positioning during robotic hand construction. Therefore, the high DOF is essential in providing ample motion primitives, enabling robotic hands to adeptly perform diverse tasks.

Previous studies have frequently utilized pneumatic actuators for soft fingers, which rely on the application of

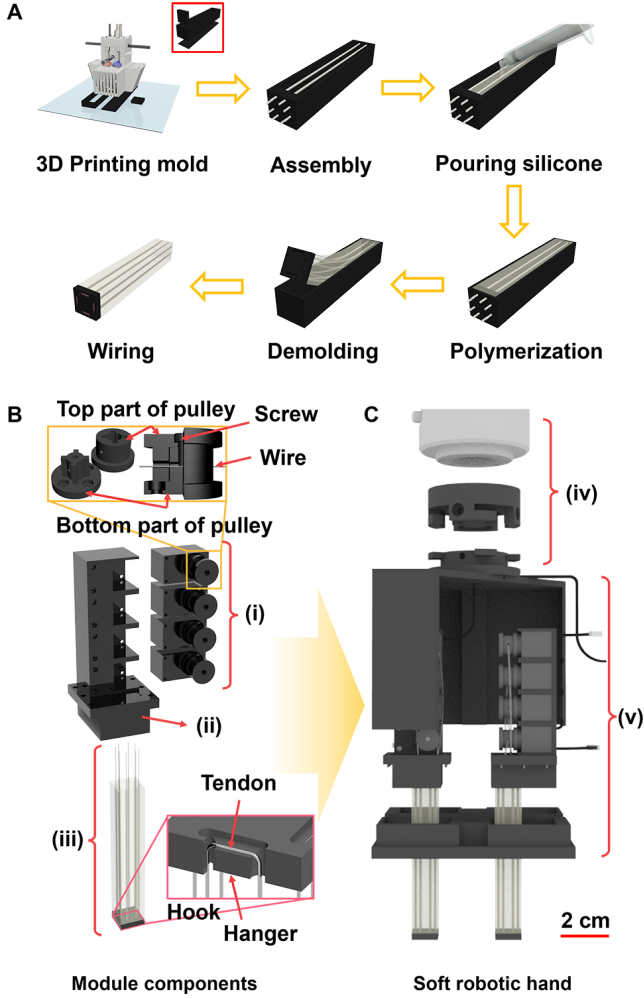


Fig. 2. Fabrication and design schematic of soft finger module and soft robotic hand. On the left, the main components of the soft finger module are presented. (A) Fabrication process of the soft finger. (B) Structure of the soft finger module. (i) Motor set with pulley. (ii) Docker. (iii) Soft finger with super-elastic tendons and the hook. (C) Structure of the soft hand. (iv) Adapting parts between collective robotic arm and the platform cover of our robotic hand. (v) Platform and platform cover with soft finger modules connected with motor cables.

pneumatic pressure within patterned air chambers in order to drive actuation [9]–[13]. Although these actuators can produce significant forces, increasing the DOF in pneumatic fingers can complicate their internal structure and require additional tethers and larger actuator bodies. Additionally, the need for a heavy control unit, such as an air cylinder, pump, and regulators further limit their effective integration into diverse robotic hands. Several studies reported a modular approach to constructing diverse forms of a robotic hand with pneumatic actuators, but they require an air control system that occupies a significant volume and adds weight, making it difficult to seamlessly integrate pneumatic actuators into a single module without heavy tethering [4], [14]–[16].

In contrast, tendon-driven actuators allow for straightforward adjustments to the DOF through simple design modifications that integrate additional tendons [2], [17], [18].

Tendons require less space than air chambers in pneumatic actuators, which allows the use of lighter control systems and simplified tethering with minimal wiring [19]–[22]. Although tendon-driven actuators offer clear advantages in terms of modularity and system integration, the selection of the actuation method alone is insufficient to achieve optimal robotic hand performance. Beyond the choice of actuator type, the overall design must also address the manner in which multiple actuated fingers collectively function as a coordinated system.

The configuration of the soft fingers is of pivotal importance in determining the cooperative motion capabilities of multi-gait robotic hands. The dexterity of a single soft finger is insufficient for evaluating and designing the cooperative motion of multiple soft fingers. This is because it typically depends on intrinsic material characteristics or internal design without consideration of the coordination between the fingers [23]. Consequently, the motion capabilities of robotic hands are closely tied to the arrangement of the soft fingers. This arrangement determines the workspace allocation for each finger and its position [15], [24], [25]. Therefore, a comprehensive design approach must consider not only the characteristics of individual fingers but also the strategic design of their arrangement to improve the performance of the hand for specific tasks [1], [2], [14].

Conventional soft robotic hands, which are typically characterized by monolithic structures or a limited number of components, present significant challenges in adapting the hand to versatile tasks. This often requires a comprehensive redesign of the hand. Despite the existence of numerous soft robotic hands with varying DOFs and diverse finger configurations, only a few studies have tackled challenges of design dependency [3]. Some research has investigated the potential of adaptable shape platforms and modularized fingers to allow for easier alterations in finger arrangement and thereby reducing the need for extensive redesign [15], [26]–[28].

To address the limitations in current soft robotic hand design, there is a clear need for a systematic approach that combines the benefits of tendon-driven actuation with true modularity. The ideal solution integrates individual finger modules with their dedicated control systems, thereby eliminating the dependency on centralized, bulky control units, while enabling rapid reconfiguration of finger arrangements. This architecture supports the adaptation of hand configurations to suit particular tasks without requiring fundamental redesigns, bridging the gap between the flexibility offered by tendon-driven systems and the practical demands of versatile robotic applications.

This paper presents a modular system that employs tendon-driven actuators to create versatile robotic hands with high DOF and straightforward reconfigurability in a compact volume. The integration of the soft finger and driving components serves to reduce the complexity of the internal structure while maintaining a high DOF. The system is composed of two primary components: a module consisting of a soft finger and driving components, and a platform to house these modules.

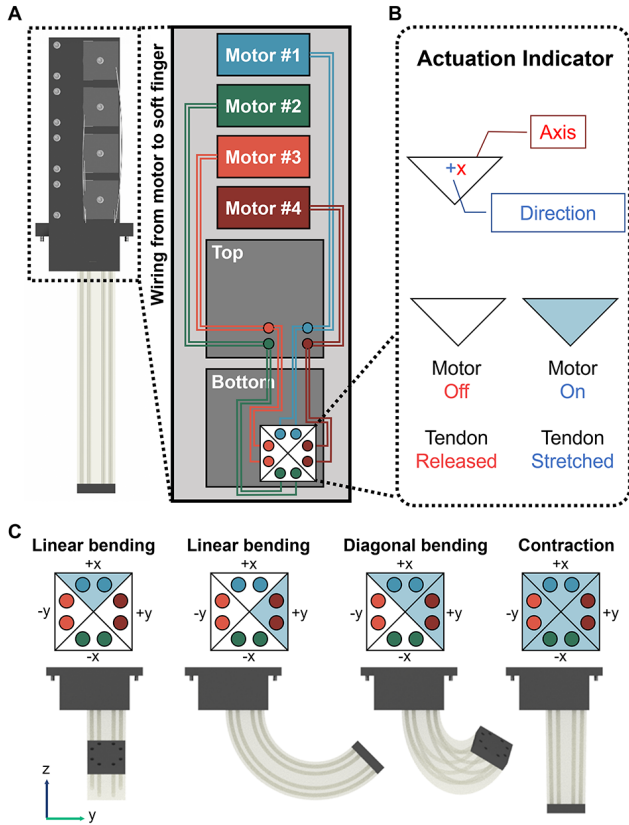


Fig. 3. Actuation mechanism of the soft finger module. (A) Schematic displaying working mechanism of the soft finger and tendon connections. (B) Actuation indicator. The working mechanism for diverse actuation modes is visualized with a triangle-shaped diagram, which serves as an actuation indicator. (C) Schematic illustrating actuation modes of the soft finger module. This diagram highlights the direction, axis, and state of tendon in response to motor operation.

The soft fingers feature a four-way tendon configuration, enabling independent control of each tendon and granting the module a high DOF. This operational mechanism expands the workspace and enhances the range of motion of robotic hands, offering high stability and adaptability across diverse hand designs.

Four distinct platform configurations have been devised with the objective of facilitating efficient manipulation in daily tasks, as depicted in Fig. 1. These configurations enable the system to perform a variety of manipulation tasks, from simple to complex, leveraging the high DOF of the modules. The modules can be swiftly reassembled on other platforms, thus enhancing adaptability to diverse tasks. To achieve sophisticated control of coordinated finger movements, we employed neural network-planned trajectories. This data-driven approach allowed us to complete intricate tasks. Furthermore, we delineate both the motion primitives of the module and examine the cooperative manipulation capabilities of the robotic hands, subsequently discussing the results.

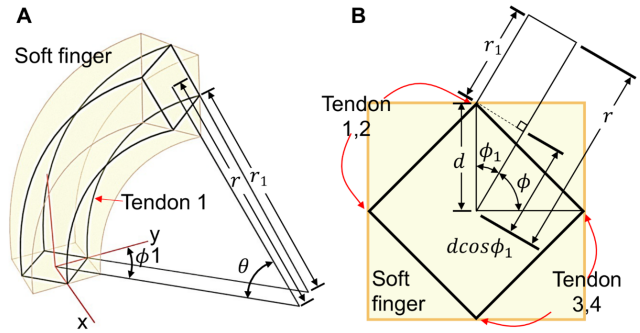


Fig. 4. Schematic representation of the arc analysis of the finger's bending deformation. (A) Isometric view of the finger bending. (B) Base of the finger from a top-down view along the z-axis.

## II. MATERIALS AND METHODS

Fig. 2A illustrates the fabrication process for the soft finger module, which integrates a silicon main body, a 3D printed plastic hook, and superelastic nitinol wire tendons (0.5 mm in diameter). The main body ( $20 \times 20 \times 120\text{mm}^3$ ) is molded using a 1:1 mixture of Ecoflex 00-30 (Smooth-on) and cured at  $60^\circ\text{C}$ . PLA molds, including the dedicated plastic hook, are fabricated via 3D printing and employed alongside temporary silicone conduits that secure the tendon pathways during curing. To enhance grip and kinematic coupling with target objects, a compliant silicone cap is applied over the plastic hook [29], [30]. After curing, the conduits are removed, and the nitinol tendons are threaded and looped around the internal hook hangers. This fabrication strategy not only ensures consistent tendon routing, but also lays the groundwork for the soft finger's multidirectional actuation and its subsequent integration into the soft robotic hand.

### A. Design of Soft Finger Module and Soft Robotic Hand

The soft finger module incorporates a motor-tendon system housed within a minimalist, 3D-printed PLA docker shown in Fig. 2B and 3A. The docker features integrated motor sockets, tendon guides, and a docking section with eight strategically placed holes that align with the tendon pathways, ensuring uniform tension and preventing tangling during operation. The motors are arranged vertically and connected via compact cables for power and communication. They drive the tendons, which are routed from the internal hook hanger through both the soft finger and the docker. Tendon routing is facilitated by 3D printed pulleys with a 7 mm radius and a 9 mm lip, which are secured with screws and enable precise, multi-directional actuation.

The soft robotic hand itself is constructed from modular components including the soft finger modules, a 3D printed platform, cover, and connector set. The platform and cover—designed with heights of 25 mm and 120 mm respectively—ensure adequate space for the modules. Once mounted on the platform, the main motor cable is routed through a central aperture in the cover. A dedicated 3D printed arm connector set, comprising an arm connector and

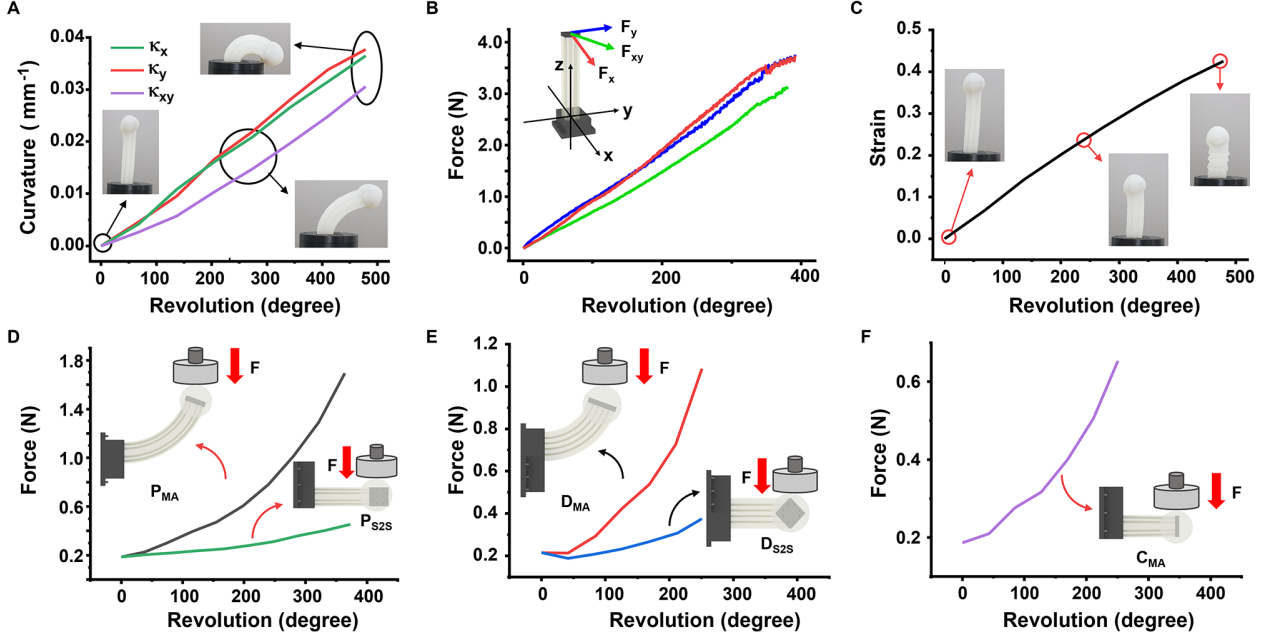


Fig. 5. Soft finger module force characterization and stiffness analysis. (A) Curvature. (B) Pushing force. (C) Compressive strain. (D, E) Stiffness measurement of plane-directional and diagonal bending actuation under external load applied in the direction of MA and S2S. (F) Stiffness measurement of contraction actuation under external load applied in the direction of MA. The notations P, D, and C represent bending direction: plane, diagonal, and compression, respectively. The subscript specifies the direction of the force.

a cover connector with an integrated cable pathway, enables secure attachment to a 6-DOF collaborative robot (Universal Robots UR-5e). This design streamlines integration while maintaining robustness and ease of assembly.

#### B. Interior Wiring and Working Mechanism

Tendons are anchored at the internal hook and routed through the soft finger from the hook to the docker, wrapping around motor pulleys where a securing screw maintains tension. Arranged in a symmetrical circular configuration, four dedicated guiding pathways ensure that each tendon corresponds to a specific motor, enabling multi-directional actuation while minimizing hysteresis.

Motor-driven tendon winding enables diverse manipulation tasks. As shown in Fig. 3A, tendon-to-motor connections allow different actuation types, while Figs. 3B and 3C use a four-division square diagram to illustrate tendon coordination and motor states. Each triangular tile in the diagram corresponds to a tendon's position on the hook, with tendons unwound in the relaxed state. Coordinated motor operations produce controlled bending, including diagonal movements and uniform contraction, with bending angles proportional to motor revolutions.

### III. CHARACTERIZATION OF SOFT FINGER MODULE

#### A. Bending Performance Analysis

Figure 4 shows the tendon routing and arc fitting used to extract the backbone curvature  $\kappa$ . Let  $l_0$  be the neutral tendon length and  $\omega = [\omega_1, \omega_2, \omega_3, \omega_4]^\top$  the motor rotations.

Defining  $\Delta\omega_x = \omega_3 - \omega_1$  and  $\Delta\omega_y = \omega_4 - \omega_2$ , the closed-form mapping is

$$\kappa(\omega) = \frac{r_p (\omega_1 - 3\omega_2 + \omega_3 + \omega_4) \sqrt{\Delta\omega_x^2 + \Delta\omega_y^2}}{d (4l_0 - r_p \sum_{i=1}^4 \omega_i) \Delta\omega_y} \quad (1)$$

where  $r_p$  is the pulley radius and  $d$  the tendon-to-axis offset. This analytical mapping provides a physically interpretable baseline, serving as an optional reference for controller tuning or model validation.

Fig. 5A illustrates the bending deformation along the x, y, and diagonal axes. Curvatures  $\kappa_x$ ,  $\kappa_y$ ,  $\kappa_{xy}$  estimated by tracing a circle along the centerline. It increases linearly with motor rotation up to 480°.  $\kappa_x$ ,  $\kappa_y$  are approximately 0.0365 mm⁻¹ and 0.0377 mm⁻¹, while  $\kappa_{xy}$  is lower at 0.0306 mm⁻¹, likely due to increased stress during edge-direction bending.

#### B. Pushing Force Evaluation

A customized setup with a 3D printed module holder and a universal testing machine (UTM, INSTRON 3343) is used to measure bending forces along the x, y, and diagonal axes as the tendon pulley rotated. In Fig. 5B, motor rotations reached up to 391° for the x and y axes and 381° for the diagonal, yielding maximum forces of 3.75 N, 3.74 N, and 3.14 N, respectively.

#### C. Contraction Performance Analysis

In Fig. 5C, we also evaluate the compressive strain of the soft finger module using the UTM. During testing, all tendons are pulled simultaneously along the z-axis at the

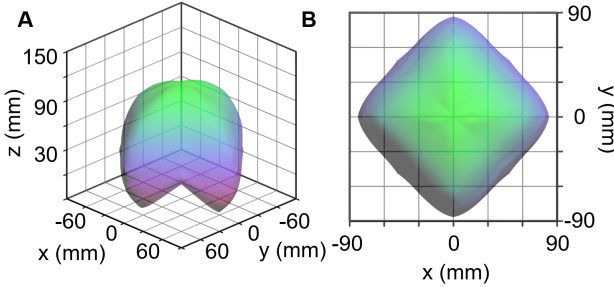


Fig. 6. Workspace of the soft finger module. (A) Isometric view and, (B) top view in 3D workspace.

same rate. The compression plate is positioned slightly above the fingertip, and we measure the displacement of plate until the force of 0.05 N is detected, with a motor revolution range of 0 to 480 degrees. The finger shows a 42.6% contraction ultimately. Due to the superelasticity and incompressibility of the tendons, the length change from contraction remains consistent, with strain linearly increasing alongside the motor revolution.

#### D. Stiffness Analysis

Stiffness variations are assessed by recording the force required to displace the soft finger by 5 mm under both bending and contraction conditions using UTM compression tests. In bending experiments, forces measured along the main axis (MA) are significantly higher than those measured along the lateral (S2S) direction. For instance, during planar bending at 363°, the MA force is 1.70 N, which is 3.73 times greater than the lateral force; similarly, in diagonal bending at 251°, the MA force is 1.09 N, 2.89 times that of the lateral force. During contraction, the MA force reaches 0.654 N at 251° as shown in Figs. 5D, 5E, and 5F.

#### E. 3D Workspace

Fig. 6 shows that the soft finger module achieves nearly omnidirectional performance within the hand. Using a piecewise constant curvature model, its 3D workspace is computed based on motor-induced bending (x, y, and diagonal) and contraction (z-axis). The workspace has a mushroom-like shape, with an x–y reach of 86.28 mm (71.9% of the original length) due to tendon-induced compression. A square-like top view reveals that diagonal bending results in a shorter z-axis reach of 68.71 mm (57.3% of the original length), yet overall, the design maintains excellent dexterity.

#### F. Planning Motion Primitive using Neural Network

Similar to Bern et al [31] we employ a neural network to model the kinematics of a soft robot to follow the target trajectory and plan a useful motion primitive. A paired dataset of actuation and position of end-effector is collected using the motion capture device (Optitrack flex-13), amounting to 3K entries. A forward kinematics function  $K$  is identified to map actuation (i.e. degree of rotation of motors) to position. The actuation sequence  $a_{\text{seq}} = \{a_1, a_2, \dots, a_n\}$  to achieve desired trajectory  $x_{\text{des}} = \{x_1, x_2, \dots, x_n\}$  can be found

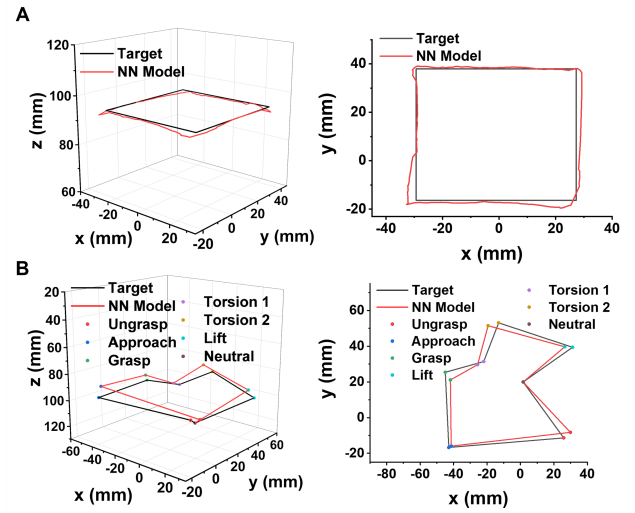


Fig. 7. Trajectory following for given target and actual trajectory measured when deployed. (A) A trajectory to draw square. (B) A trajectory to rotate a bottle cap.

TABLE I  
RMSE OF PLANNING MOTION PRIMITIVES

Trajectory type	Drawing square (mm)	Rotating bottle cap (mm)
RMSE of x	2.236	3.582
RMSE of y	1.446	2.073
RMSE of z	1.890	4.420
Mean of Euclidean distance	3.102	5.086
RMSE of Euclidean distance	3.266	6.055

by solving Eq. (2), where  $n$  is number of waypoints for given trajectory. As the Jacobian  $\frac{\partial K}{\partial a}$  is obtained from the autogradient framework, in our case Pytorch [32], Eq. (2) is solved with the Limited-memory BFGS (L-BFGS) algorithm [33].

$$a_i = \arg \min_a \|K(a) - x_i\|^2 \quad (2)$$

The model is tested on two target trajectories: drawing a square and rotating a bottle cap, as depicted in Fig. 7A and B, respectively. The trajectory of the soft finger, guided by a neural network model, is captured and analyzed using motion tracking. Table I details root-mean-square-error (RMSE) values for target trajectories. The mean and RMSE of the Euclidean distance remain within 1.5% and 2.1% for square drawing and bottle cap rotation, respectively, demonstrating the precision of the motion primitives.

## IV. EXPERIMENTS AND DISCUSSION

Our experimental evaluation explores four distinct configurations of the soft robotic hand. Each configuration is tailored to address specific challenges in dexterous manipulation. Configuration 1 integrates a single soft finger with a UR-5e arm under neural network control. The configuration executes precise letter writing, using linear motions for

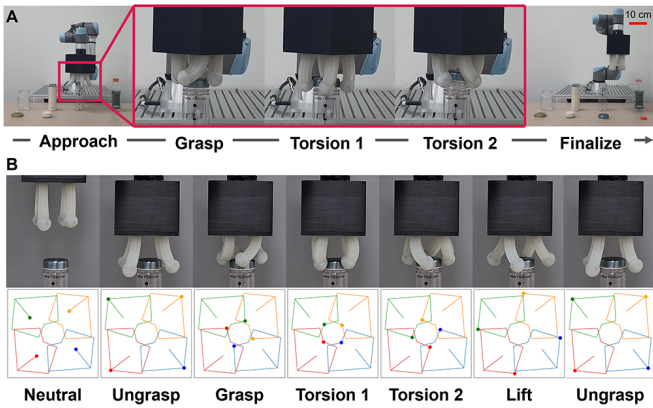


Fig. 8. Bottle screw performances of Configuration 3. (A) Rapid and precise manipulation for opening four bottle caps with varying cap types using Configuration 3. (B) Sequence illustrating the precise manipulation process for twisting a bottle cap.

straight strokes and controlled, tangent-based bending for curves. Configuration 2 adopts a three-finger arrangement to robustly grip and manipulate everyday objects demonstrating both strength and gentle precision. Configuration 3 and Configuration 4 then tackle progressively more complex tasks, as detailed in the following sections. Further performance nuances and real-time demonstrations are provided in the supplementary video.

#### A. Rotating a Bottle Cap with Configuration 3

Configuration 3, which features four radially oriented fingers, excels in tasks such as opening and closing bottle caps, as illustrated in Fig. 8. Fig. 8A exhibits that Configuration 3 successfully opens four bottle caps of different sizes (38 to 70 mm) and textures (smooth and rough), with UR-5e's assistance for positioning. Fig. 8B illustrates the actuation sequence used to open a bottle cap, which is executed using the trained model depicted in Fig. 7B. The soft hand flexes clockwise to maximize the unscrewing range, firmly grasps the cap, and then flexes counterclockwise to release it.

Opening a bottle cap using in-hand manipulation is challenging due to the extremely tight tolerances involved. Furthermore, both rotational and linear motions are required to successfully disengage the threaded cap, making a simple twist insufficient [34]. The flexibility of the soft finger and high DOF reduce these challenges by enabling both contraction and flexion. When combined with the proper configuration and precise trajectory tracking, the system successfully opens the various caps. Interestingly, fastening the cap back is even more challenging [34]. However, if the actuation sequence is simply reversed, the proposed soft hand can close the cap without requiring additional computations or control adjustments. Performance nuances are available in the supplementary video.

#### B. Spreading and Re-orientating Tasks with Configuration 4

Configuration 4, which features linearly arranged fingers, excels in tasks that involve finger or palm manipulations, such as petting, tipping, and scratching. We demonstrate

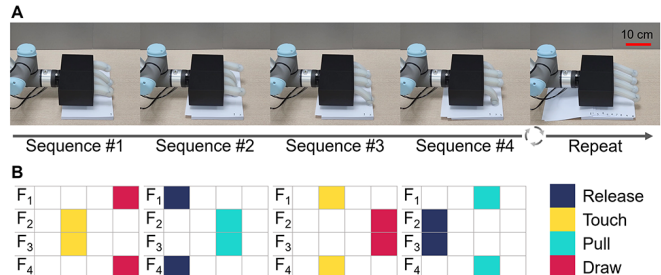


Fig. 9. Manipulation performances of Configuration 4. (A) The soft hand spreads precisely a pile of paper, one by one. (B) Actuation pattern table indicates the finger gait pattern for the task.

counting stacks of letter paper as illustrated in Fig. 9A. The paper counting task involves finger-based manipulations to accurately count each sheet in a numbered stack, combining tipping and scratching motions. In Fig. 9B, a repetitive four-step sequence such as release, touch, pull, and draw is designed to manage friction between paper sheets. In this sequence, “Release” prepares the fingers for contact, “touch” involves a moderate bend to engage the paper, “pull” is a stronger bend for pulling the sheet, and “draw” fully contracts the fingers to prevent interference after the pull.

The task is challenging due to the thin, lightweight nature of sheets and static-caused adhesion between sheets. This coordinated approach ensures precise counting of each sheet without any slippage or miscounts. This demonstrates Configuration 4’s accuracy in complex finger-based tasks, showing both the force and shear maintained within a narrow range throughout the pulling process.

## V. CONCLUSIONS AND FUTURE WORK

This paper presents a tendon-driven soft finger with high DOF as the basis for a versatile, modular soft robotic hand that can be tailored to specific tasks. The design uses a tendon pulling mechanism for intuitive manipulation and offers diverse actuation modes with a wide workspace. Four representative platforms are developed to cover a range of motions, from simple grasping to complex actions. Configuration 1 demonstrates advanced logo-writing, Configuration 2 excels in gentle grasping of diverse objects, while Configuration 3 and 4 open and close bottle caps and count paper sheets. These demonstrations highlight the system’s precision and efficiency in performing dexterous hand manipulations.

Looking forward, we see substantial potential for our module to enhance the capabilities of soft robotic hands. Future enhancements include increasing the finger’s DOF with longitudinal expansion actuation and integrating sensing capabilities for closed-loop feedback. In addition, we plan to develop adaptive platform configurations that automatically adjust to specific tasks, ensuring optimal performance in diverse dexterous manipulation. This will improve adaptability and enable more intelligent interactions. This may open up new possibilities for innovative and efficient solutions within the realm of soft robotics.

## REFERENCES

- [1] D. Rus and M. T. Tolley, "Design, fabrication and control of soft robots," *Nature*, vol. 521, no. 7553, pp. 467–475, 2015.
- [2] C. Laschi, B. Mazzolai, and M. Cianchetti, "Soft robotics: Technologies and systems pushing the boundaries of robot abilities," *Science robotics*, vol. 1, no. 1, p. eaah3690, 2016.
- [3] H. Wang, M. Totaro, and L. Beccai, "Toward perceptive soft robots: Progress and challenges," *Advanced Science*, vol. 5, no. 9, p. 1800541, 2018.
- [4] S. Abondance, C. B. Teeple, and R. J. Wood, "A dexterous soft robotic hand for delicate in-hand manipulation," *IEEE Robotics and Automation Letters*, vol. 5, pp. 5502–5509, 10 2020.
- [5] K. Suzumori, S. Iikura, and H. Tanaka, "Development of flexible microactuator and its applications to robotic mechanisms," in *Proceedings. 1991 IEEE International Conference on Robotics and Automation*. IEEE, 1991, pp. 1622–1627 vol.2.
- [6] U. Kim, D. Jung, H. Jeong, J. Park, H.-M. Jung, J. Cheong, H. R. Choi, H. Do, and C. Park, "Integrated linkage-driven dexterous anthropomorphic robotic hand," *Nature communications*, vol. 12, no. 1, p. 7177, 2021.
- [7] J. Zhang, Y. Li, Z. Kan, Q. Yuan, H. Rajabi, Z. Wu, H. Peng, and J. Wu, "A preprogrammable continuum robot inspired by elephant trunk for dexterous manipulation," *Soft Robotics*, vol. 10, no. 3, pp. 636–646, 2023.
- [8] Z. Xie, A. G. Domel, N. An, C. Green, Z. Gong, T. Wang, E. M. Knubben, J. C. Weaver, K. Bertoldi, and L. Wen, "Octopus arm-inspired tapered soft actuators with suckers for improved grasping," *Soft robotics*, vol. 7, no. 5, pp. 639–648, 2020.
- [9] W. Hu, R. Mutlu, W. Li, and G. Alici, "A structural optimisation method for a soft pneumatic actuator," *Robotics*, vol. 7, no. 2, p. 24, 2018.
- [10] A. Firouzeh, M. Salerno, and J. Paik, "Soft pneumatic actuator with adjustable stiffness layers for multi-dof actuation," in *2015 IEEE/RSJ International Conference on Intelligent Robots and Systems (IROS)*. IEEE, 2015, pp. 1117–1124.
- [11] C. Suh, J. C. Margarit, Y. S. Song, and J. Paik, "Soft pneumatic actuator skin with embedded sensors," in *2014 IEEE/RSJ International Conference on Intelligent Robots and Systems*. IEEE, 2014, pp. 2783–2788.
- [12] H. Li, J. Yao, P. Zhou, X. Chen, Y. Xu, and Y. Zhao, "High-force soft pneumatic actuators based on novel casting method for robotic applications," *Sensors and Actuators A: Physical*, vol. 306, p. 111957, 2020.
- [13] K. Suzumori, S. Iikura, and H. Tanaka, "Flexible microactuator for miniature robots," in *[1991] Proceedings. IEEE Micro Electro Mechanical Systems*. IEEE, 1991, pp. 204–209.
- [14] F. Schmitt, O. Piccin, L. Barbé, and B. Bayle, "Soft robots manufacturing: A review," *Frontiers in Robotics and AI*, vol. 5, p. 84, 2018.
- [15] C. B. Teeple, R. C. S. Louis, M. A. Graule, and R. J. Wood, "The role of digit arrangement in soft robotic in-hand manipulation," in *2021 IEEE/RSJ International Conference on Intelligent Robots and Systems (IROS)*. IEEE, 2021, pp. 7201–7208.
- [16] C. B. Teeple, G. R. Kim, M. A. Graule, and R. J. Wood, "An active palm enhances dexterity of soft robotic in-hand manipulation," in *2021 IEEE International Conference on Robotics and Automation (ICRA)*, 2021, pp. 11 790–11 796.
- [17] P. Wang, Z. Tang, W. Xin, Z. Xie, S. Guo, and C. Laschi, "Design and experimental characterization of a push-pull flexible rod-driven soft-bodied robot," *IEEE Robotics and Automation Letters*, vol. 7, no. 4, pp. 8933–8940, 2022.
- [18] A. K. Mishra, E. Del Dottore, A. Sadeghi, A. Mondini, and B. Mazzolai, "Simba: Tendon-driven modular continuum arm with soft reconfigurable gripper," *Frontiers in Robotics and AI*, vol. 4, 2017. [Online]. Available: <https://www.frontiersin.org/articles/10.3389/frobt.2017.00004>
- [19] H. Lee, Y. Jang, J. K. Choe, S. Lee, H. Song, J. P. Lee, N. Lone, and J. Kim, "3d-printed programmable tensegrity for soft robotics," *Science Robotics*, vol. 5, no. 45, p. eaay9024, 2020.
- [20] J.-H. Lee, Y. S. Chung, and R. Hugo, "Long shape memory alloy tendon-based soft robotic actuators and implementation as a soft gripper," *Scientific Reports*, vol. 9, 08 2019.
- [21] A. L. Gunderman, J. A. Collins, A. L. Myers, R. T. Threlfall, and Y. Chen, "Tendon-driven soft robotic gripper for blackberry harvesting," *IEEE Robotics and Automation Letters*, vol. 7, no. 2, pp. 2652–2659, 2022.
- [22] J. M. Bern, F. Zargarbashi, A. Zhang, J. Hughes, and D. Rus, "Simulation and fabrication of soft robots with embedded skeletons," in *2022 International Conference on Robotics and Automation (ICRA)*, 2022, pp. 5205–5211.
- [23] L. A. Al Abeach, S. Nefti-Meziani, and S. Davis, "Design of a variable stiffness soft dexterous gripper," *Soft robotics*, vol. 4, no. 3, pp. 274–284, 2017.
- [24] K. Or, M. Tomura, A. Schmitz, S. Funabashi, and S. Sugano, "Interpolation control posture design for in-hand manipulation," in *2015 IEEE/SICE International Symposium on System Integration (SII)*. IEEE, 2015, pp. 187–192.
- [25] S. Puhlmann, J. Harris, and O. Brock, "Rbo hand 3: A platform for soft dexterous manipulation," *IEEE Transactions on Robotics*, vol. 38, no. 6, pp. 3434–3449, 2022.
- [26] W. Huang, J. Xiao, and Z. Xu, "A variable structure pneumatic soft robot," *Scientific Reports*, vol. 10, 12 2020.
- [27] K. C. Galloway, K. P. Becker, B. Phillips, J. Kirby, S. Licht, D. Tchernev, R. J. Wood, and D. F. Gruber, "Soft robotic grippers for biological sampling on deep reefs," *Soft robotics*, vol. 3, no. 1, pp. 23–33, 2016.
- [28] A. S. Morgan, K. Hang, B. Wen, K. E. Bekris, and A. M. Dollar, "Complex in-hand manipulation via compliance-enabled finger gaiting and multi-modal planning," *CoRR*, vol. abs/2201.07928, 2022. [Online]. Available: <https://arxiv.org/abs/2201.07928>
- [29] M. R. Cutkosky and P. K. Wright, "Friction, stability and the design of robotic fingers," *The International Journal of Robotics Research*, vol. 5, no. 4, pp. 20–37, 1986.
- [30] B. W. McInroe, C. L. Chen, K. Y. Goldberg, K. Y. Goldberg, R. Bajcsy, and R. S. Fearing, "Towards a soft fingertip with integrated sensing and actuation," in *2018 IEEE/RSJ International Conference on Intelligent Robots and Systems (IROS)*, 2018, pp. 6437–6444.
- [31] J. M. Bern, Y. Schnider, P. Banzet, N. Kumar, and S. Coros, "Soft robot control with a learned differentiable model," in *2020 3rd IEEE International Conference on Soft Robotics (RoboSoft)*, 2020, pp. 417–423.
- [32] A. Paszke, S. Gross, F. Massa, A. Lerer, J. Bradbury, G. Chanan, T. Killeen, Z. Lin, N. Gimelshein, L. Antiga, A. Desmaison, A. Kopf, E. Yang, Z. DeVito, M. Raison, A. Tejani, S. Chilamkurthy, B. Steiner, L. Fang, J. Bai, and S. Chintala, *PyTorch: An Imperative Style, High-Performance Deep Learning Library*. Red Hook, NY, USA: Curran Associates Inc., 2019.
- [33] D. C. Liu and J. Nocedal, "On the limited memory bfgs method for large scale optimization," *Mathematical programming*, vol. 45, no. 1, pp. 503–528, 1989.
- [34] C. Jiao, L. Zhang, X. Su, J. Huang, Z. Bing, and A. Knoll, "Task-based compliance control for bottle screw manipulation with a dual-arm robot," *IEEE Transactions on Industrial Electronics*, vol. 71, no. 2, pp. 1823–1831, 2023.